

Fabrication and characterization of ZnO/Si Heterojunction by Laser Ablation for Solar Cell Application

Ban R. Ali*

Department of Physics, College of Science, Mustansiriyah University, Baghdad, Iraq

*Author email: banrasheed2003@uomustansiriyah.edu.iq

Article Info

Submitted
23/12/2018

Accepted
04/03/2019

Published
01/10/2019

Abstract

Nanoparticles of semiconductor material have got more interest due to their desirable properties and applications in different areas. In this study Zinc Oxide Nanoparticles (ZnO NPs) were synthesized using laser ablation in water by applying (1600 pulses) of Nd- YAG laser ($\lambda = 1064 \text{ nm}$). The crystal structure and morphology of the synthesized ZnO NPs were investigated using X-Ray diffraction, atomic force microscope (AFM), optical microscope image, and optical properties characterized using UV-Visas well as FTIR spectroscopy. The investigation revealed high purity of the ZnO NPs thin film prepared with a regular and homogeneous semi-spherical shape nanoparticles distributed on the substrate surface with size around 50nm. The optical properties show energy band gap of (1.5 eV and 4eV) respectively. I-V characteristics have been studied for the heterojunction structure of (Ag/ZnO/Si/Al) indicates that this heterojunction could be used as a solar cell with efficiency about 10.9%.

Keywords: ZnO, Laser Ablation, XRD, AFM, Optical Properties.

الخلاصة

تحضير خلية شمسية من تركيب المفروق الهجين (ZnO/Si) بواسطة الاستئصال الليزريلقد اكتسبت الاجسام النانوية للمواد شبه الموصله المزيد من الاهتمام بسبب خواصها المرغوبه في العديد من التطبيقات في مختلف المجالات . في هذه الدراسه تم الحصول التركيب النانوي لمادة اوكسيد الزنك باستخدام تقنيه التقشير بالليزر داخل الماء وذلك من خلال تسليط (1600) نبضه لليزر النيوديميوم-ياك ذو الطول الموجي (1064 نانومتر).

التركيب البلوري لمادة اوكسيد الزنك النانويه المحضرة تم دراسته باستخدام الاشعة السينية , ومكروسكوب القوة الذرية ,دراسه الصورة البصرية بالميكروسكوب. اما الخصائص البصريه فقد تم دراستها باستخدام مطياف الاشعه المرئيه وفوق البنفسجية ومطياف الاشعه تحت الحمراء. ولقد اثبتت هذه الدراسات نقاوة عاليه لغشاء اوكسيد الزنك المحضر مع ترسيب منتظم ومتجانس للاجسام النانويه التي كانت باشكال شبه كرويه على سطح الركيزة باحجام بحدود (50 نانومتر). الخصائص الكهربيائيه التي تم دراستها في هذا البحث للتركيب الهجينالمحضر تشير الى انه هذا التركيب ممكن استخدامه كخليه شمسيه وبكفاءه حوالي 10,9 %

Introduction

For its high transparency in visible range, high absorption, and nearly optimum band gap energy, Zinc Oxide (ZnO) has most motivated material as a conductive oxide for many applications[1-4]. ZnO thin films one the most intensive material that has demonstrated significant interest in modern industry [5-7]. Several studies have been done in the last few years about their potential applications in transparent electrode display, windows layers in solar cells, ultraviolet laser emission photo detectors, light emitting diodes, laser diodes, gas sensing, and bio sensor [8-11]. Since the morphology of the

synthesized nanoparticles depend on the preparation of nanoparticles method, therefore it is important to get optimum conditions for synthesizing ZnO nanoparticles and controlling on the crystals morphology such as size, shape and various parameters that effect on the ZnO properties. Many techniques were used for synthesizing ZnO NPs such as thermal oxidation [12], chemical vapor deposition [13], Sol-Gel method [14], molecular beam epitaxial [15], and laser ablation [16]. Pulsed laser ablation in liquid among various methods (PLAL) has attracted attention due to its simplicity, does not require vacuum environment [17] and the con-

trolling on the size and shape of the synthesized nanoparticles. PLAL is essential technique to get optimum conditions for fabrication highly oriented and transparent ZnO thin films [17, 18]. In this article, we use laser ablation in water to get pure ZnO NPs, and drop casting method for preparation a well-covered and homogeneous ZnO NPs thin film. The crystal structure and morphology ZnO NPs thin films were investigated by XRD, AFM, FTIR and the optical properties were studied for the preparation thin films.

Experimental

For synthesizing Zinc Oxide nanoparticles, laser ablation were used by applying (1600 pulses) of Nd-YAG laser ($\lambda = 1064$ nm pulse duration = 7ns and energy = 500 mJ) that focused on the Zinc target of purity (99.99 %) which immersed in distilled water at room temperature. Figure (1) shows the experimental system for the laser ablation.

The synthesized ZnO NPs solution were deposited on a glass substrate using drop casting method to get the ZnO NPs thin films. X-Ray analysis using (XRD -6000 from shimadzo) used to investigate the structural properties of the ZnO NPs thin films. Figure (2) and the calculation data in table (1) illustrate the XRD results obtained. Atomic force microscopy (AFM) (AA 3000 scanning probe Microscope) is used to study the morphology, nanoparticles properties and size of the prepared thin film. Figure (3) shows the AFM images. Optical microscope is another technique used to investigate the thin films morphology and shown in figure (4). FTIR spectroscopy is used to scan using FT-IR spectrometer. The scanned data in the range ($600-4000\text{ cm}^{-1}$) was illustrated in figure (5). The optical properties of the synthesized colloidal ZnO NPs were studied using (UV-Vis) spectrophotometer from VARIAN) and figures (6) and (7) demonstrate the optical properties.

Silicon wafer thin films were chemically cleaned and the substrates were divided into (1.5×1.5 cm) areas. Thermal deposition was used to deposit ZnO NPs on silicon substrate to obtain the ZnO/Si heterojunction. Ohmic contact was deposited using Aluminum for back

contact and silver for front contact. (I-V) characteristics under forward and reverse bias of (Ag/ZnO/Si/Al) were studied. The reverse (I-V) characteristics of the heterojunction measured under dark and illumination of ($41\mu\text{W}/\text{cm}^2$) tungsten lamp. Figures (8, 9, and 10) illustrate the I-V characteristics.

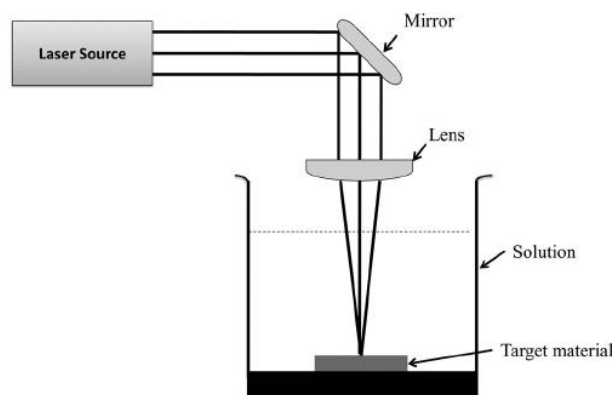


Figure (1): Experimental setup of nanoparticles synthesis by pulsed laser ablation in liquid.

Results and Discussion

The synthesized nanoparticles that deposited on a glass substrate have been characterized by its diffractometer. XRD pattern of the deposited thin film for diffraction angles (from 10° to 80°) is illustrated in figure (2). which show nine peaks on the diffraction angles ($2\theta = 31.763, 34.412, 36.246, 47.538, 56.59, 62.8505, 66.3639, 67.933, 69.08$ degree) corresponding to miller indices (hkl= 100, 002, 101,102, 110, 103, 200,112 and 201) respectively. The most intense, sharp and strong peak at (36.2469 degree) attributed to (hkl = 101). The peaks agree with the standard spectrum (PDF card -ZnO -00 -036 -145). The nanostructure was polycrystalline with a hexagonal form and there is no any trace of another structure. So, diffraction peaks corresponding to the impurity were not found in the XRD pattern. This means high purity of the thin film. The average crystalline size was ($D=47.266$ nm) and it was calculated using Scherrer's equation [18].

$$D = (0.9\lambda)/(\beta \cos\theta) \quad (1)$$

Where $\lambda = 1.5405 \text{ \AA}$ is X- Ray wavelength. β is the full width at half maximum. θ is the diffraction angle. The average micro strain (η) was

found to be $(0.000609 \text{ lin}^{-2} \cdot \text{m}^{-4})$ and the average dislocation density ($\delta = 0.000449 \text{ lin} \cdot \text{m}^{-2}$). Both η and δ were calculated from equations (2, 3) respectively [18]:

$$\eta = \beta \cos \theta / 4 \quad (2)$$

$$\delta = 1/D^2 \quad (3)$$

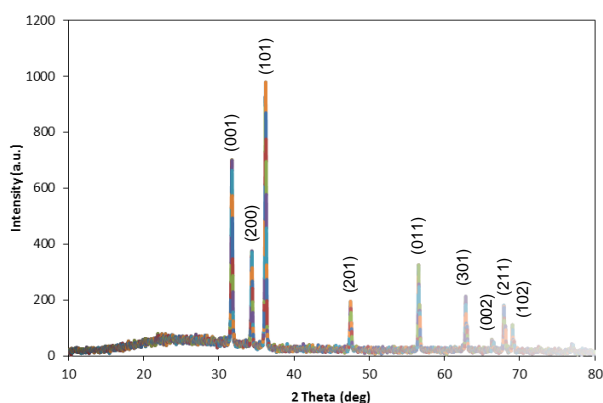


Figure (2): XRD pattern of The ZnO thin film.

Table (1): The obtained XRD analysis results for ZnO NPs thin films.

2θ (deg)	hkl	β (deg)	D (nm)	δ (lin. m ⁻²)	η (line ⁻² ·m ⁻⁴)
31.76	100	0.178	44.65	5.01×10 ⁻⁴	7.5×10 ⁻⁴
34.41	002	0.157	50.22	3.96×10 ⁻⁴	6.58×10 ⁻⁴
36.24	101	0.168	46.90	4.54×10 ⁻⁴	6.97×10 ⁻⁴
47.53	102	0.165	45.88	4.75×10 ⁻⁴	6.61×10 ⁻⁴
56.59	110	0.146	50.07	3.99×10 ⁻⁴	5.61×10 ⁻⁴
62.85	103	0.151	46.92	4.54×10 ⁻⁴	5.62×10 ⁻⁴
66.36	200	0.143	48.49	4.25×10 ⁻⁴	5.23×10 ⁻⁴
67.93	112	0.153	44.74	4.99×10 ⁻⁴	5.57×10 ⁻⁴
69.08	201	0.144	47.49	4.43×10 ⁻⁴	5.17×10 ⁻⁴

Figure (3) shows the 3D-AFM image and granularity accumulation distribution chart of ZnO NPs. We can realize that the substrate surface is well covered with semispherical shape nanoparticles that arranged as a homogeneous and uniform shape on the substrate surface. The average green size, Roughness average, and root mean square has been calculated using (Imager 4.62 software) and it was (51.09, 0.13, 0.152 nm) respectively. Particle size obtained from the AFM results is higher than that which calculated from XRD analysis because XRD technique depends on the size defect free volume, while the degree of the crystal defect

don't take into account in AFM Granularity accumulation distribution chart [19].

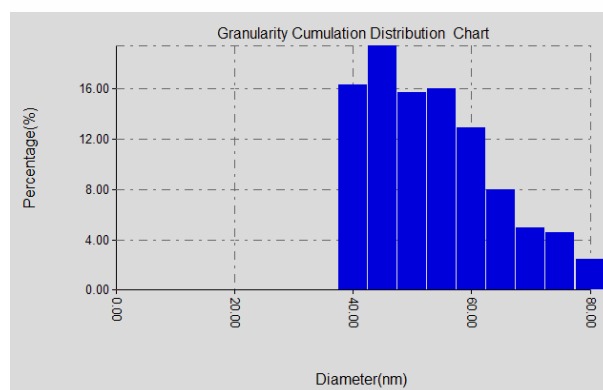
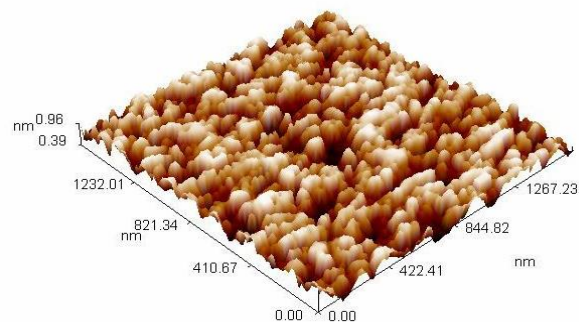


Figure (3): 3-D AFM image and granularity accumulation distribution chart.

Figure (4) illustrate the microscope image under magnification of (M=1000x). It is obvious from this figure that the surface of the glass substrate has high order covered of ZnO NPs with a regular and homogeneous distribution and no cracks or breakdowns on the substrate surface. The thin film surface was clear from any impurities or glass particles and the color consistencies indicate to the low surface roughness.

FTIR is an effective way to assign the composition of the sample. Figure (5) show the IR spectrum for the ZnO NPs. FTIR spectra for the sample prepared which taken for a wave number from (600 to 4000 cm⁻¹) shows a serious absorption peaks attributed to carboxylate and Hydroxyl impurities. The first serious absorption peaks around (3500 cm⁻¹) corresponding to O-H stretching mode of hydroxyl group [20, 21].

The observed peaks between (1200-1600 cm⁻¹) are attributed to the asymmetrical and symmet-

rical stretching of the Zinc carboxylate [22]. The data obtained are good agreement with the previous results by other researchers [23, 24]. The optical microscope image, XRD analysis, and FTIR data shows high purity of the ZnO NPs thin films prepared.

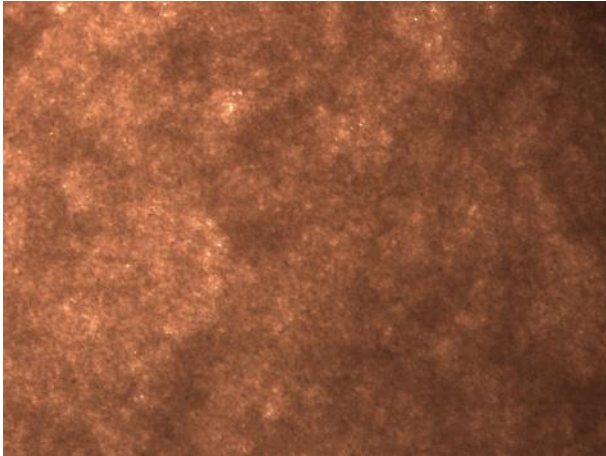


Figure (4): Optical microscope image of ZnO thin film.

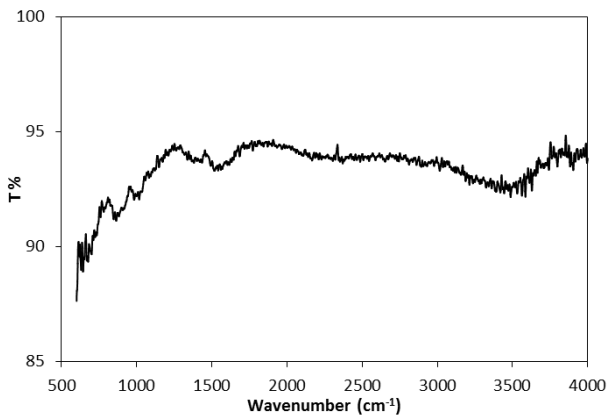


Figure (5): FTIR spectrum of the ZnO NPs.

Figure (6) shows the transmittance spectrum of the synthesized nanoparticles thin film. We can recognize from this figure that there is a high absorbance in UV region at (300nm) wavelength. The minimum transmittance occur near (400nm) near the beginning of visible region which means high absorbance at this region, with increasing the wavelength the transmittance increasing until reach it is maximum value at the wavelength (800nm) near the infrared region. This behavior indicates that this material can be used as a window in (NIR) optoelectronic devices.

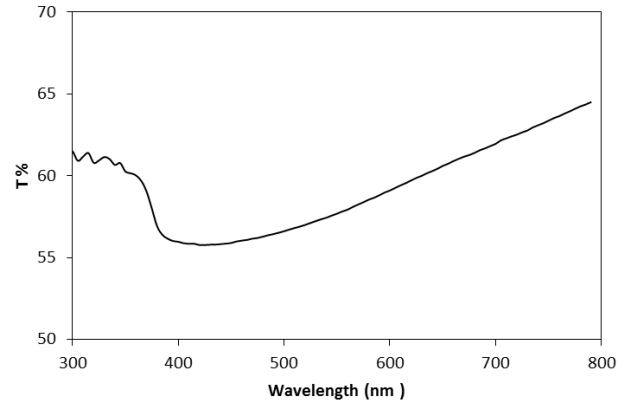


Figure (6): The transmittance versus wavelength for ZnO NPs thin film.

The energy gap can be estimated from figure (7). From this figure we can find that there are two values of the energy gap for this thin film (1.5 and 4 eV) due to the splitting of Fermi level because of the low thickness ($\sim 1 \pm 0.02 \mu\text{m}$) of the deposited thin film prepared.

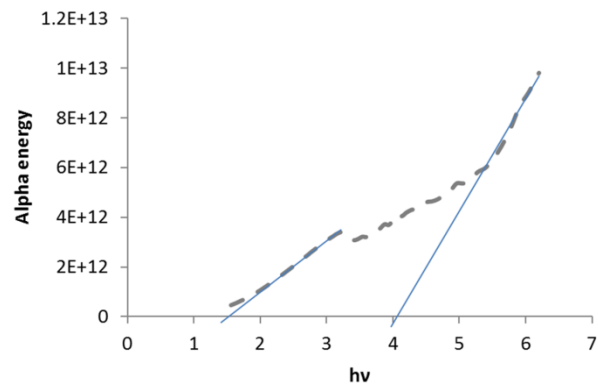


Figure (7): $(\alpha hv)^2$ versus optical energy gap of the ZnO NPs thin film.

I-V characteristics of the solar cell under forward and reverse bias at room temperature under darkness were explained in figure (8) and with illumination of $41 \mu\text{W}/\text{cm}^2$ in figure (9). It is clear from figures (8, 9) that the current value with illumination was higher than that in darkness for the same voltage, because of electron-hole generation due to light absorption [20, 25].

Which indicate the effective generation of electron-hole in the junction by incident photon?

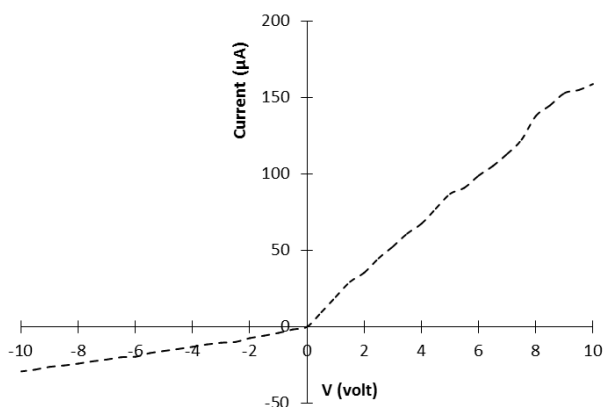


Figure (8): I-V characteristics for the ZnO/Si hetero-junction under darkness.

The relationship between I_m and V_m as a function of load resistance can be shown in figure (10). From this figure the efficiency of the Ag/ZnO/ Si-p/Al has been measured and calculated due to the equation [18]:

$$\eta = P_m/P_i = (I_m V_m)/P_i \quad (4)$$

Where P_m and P_i are the output and input power respectively. The fill factor (FF) was calculated using equation (5) [11, 17]:

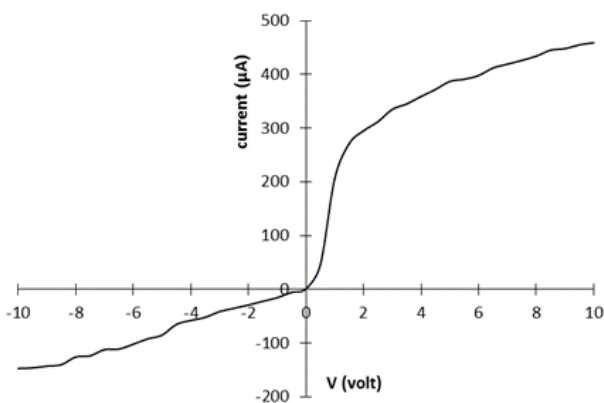


Figure (9): I-V characteristics for the Ag/ZnO/Si-p/Al hetero-junction under illumination.

$$FF = (I_m V_m)/(I_{sc} V_{oc}) \quad (5)$$

Where I_{sc} is the short circuit current and V_{oc} is the open circuit voltage. The measured V_{oc} , I_{sc} , V_m and I_m are (20 mV, 1.95 μ A, 13.5 mV, 1.3 μ A) respectively. The calculated quantum efficiency and FF was (10.9% and 45%) respectively. All the results obtained indicate

heterojunction structure of (Ag/ZnO/Si-p/Al) could be used as a solar cell.

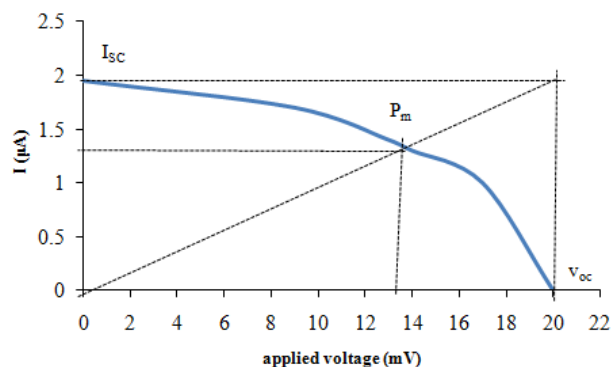


Figure (10): I-V relation of the Ag/ZnO/Si-p/Al hetero-junction.

Conclusions:

ZnO NPs which get attractive interest in many studies has applied in many applications because of it is attractive properties and one of the most important of these applications is solar cells applications.

In this article, ZnO NPs thin films with excellent structural using Laser ablation in water, which was a successful method for synthesizing ZnO nanoparticles. The synthesized ZnO NPs possess a polycrystalline hexagonal structure. These nanoparticles was uniformly distributed on a glass substrate using drop casting method which attributed high order homogeneous distribution as mentioned in the investigation that had been done in this work.

I-V characteristics for the preparation hetero-junction structure were illustrated in this article which revealed that this heterojunction could be used for solar cell applications.

References

- [1] G. QingáLu, "Enhanced photocatalytic hydrogen evolution by prolonging the lifetime of carriers in ZnO/CdS heterostructures", *Chemical communications*, pp. 3452-3454, 2009.
- [2] X. Shuai and W. Shen, "A facile chemical conversion synthesis of ZnO/ZnS core/shell nanorods and diverse metal sulfide nanotubes", *The Journal of Physical Chemistry C*, vol. 115, pp. 6415-6422, 2011.
- [3] S. Tarish, Y. Xu, Z. Wang, F. Mate, A. Al-Haddad, W. Wang, *et al.*, "Highly efficient biosensors by

- using well-ordered ZnO/ZnS core/shell nanotube arrays", *Nanotechnology*, vol. 28, p. 405501, 2017.
- [4] T.-F. Hou, A. Shanmugasundaram, M. A. Hassan, M. A. Johar, S.-W. Ryu, and D.-W. Lee, "ZnO/Cu₂O-decorated rGO: Heterojunction photoelectrode with improved solar water splitting performance", *International Journal of Hydrogen Energy*, 2018.
- [5] R. A. Chapman, R. A. Rodriguez-Davila, W. G. Vandenberghe, C. L. Hinkle, I. Mejia, A. Chatterjee, *et al.*, "Quantum Confinement and Interface States in ZnO Nanocrystalline Thin-Film Transistors", *IEEE Transactions on Electron Devices*, vol. 65, pp. 1787-1795, 2018.
- [6] C. W. Yang, H. O. SHIN, C. O. Jeong, S. K. YANG, and D. M. Lee, "Thin film transistor substrate," ed: Google Patents, 2018.
- [7] R. S. Sabry and R. S. Kammel, "Flexible Sandwich Piezoelectric Nanogenerators based ZnO Nanorods for Mechanical Energy Harvesting", *Al-Mustansiriyah Journal of Science*, vol. 29, p. 6, 2018.
- [8] V. S. Kumar and D. Kanjilal, "Influence of post-deposition annealing on structural, optical and transport properties of nanocomposite ZnO-Ag thin films", *Materials Science in Semiconductor Processing*, vol. 81, pp. 22-29, 2018.
- [9] S.-T. Kuo, W.-H. Tuan, J. Shieh, and S.-F. Wang, "Effect of Ag on the microstructure and electrical properties of ZnO", *Journal of the European Ceramic Society*, vol. 27, pp. 4521-4527, 2007.
- [10] H. J. Ali, "Boron doped Zinc Oxide for Ethanol and CO Gas Sensing", *Al-Mustansiriyah Journal of Science*, vol. 29, p. 5, 2018.
- [11] S. Tarish, Z. Wang, A. Al-Haddad, C. Wang, A. Ispas, H. Romanus, *et al.*, "Synchronous Formation of ZnO/ZnS Core/Shell Nanotube Arrays with Removal of Template for Meliorating Photoelectronic Performance", *The Journal of Physical Chemistry C*, vol. 119, pp. 1575-1582, 2015.
- [12] G. Rusu, M. Girtan, and M. Rusu, "Preparation and characterization of ZnO thin films prepared by thermal oxidation of evaporated Zn thin films", *Superlattices and Microstructures*, vol. 42, pp. 116-122, 2007.
- [13] B. Li, Y. Liu, Z. Chu, D. Shen, Y. Lu, J. Zhang, *et al.*, "High quality ZnO thin films grown by plasma enhanced chemical vapor deposition", *Journal of Applied Physics*, vol. 91, pp. 501-505, 2002.
- [14] Z. R. Khan, M. S. Khan, M. Zulfeqar, and M. S. Khan, "Optical and structural properties of ZnO thin films fabricated by sol-gel method", *Materials Sciences and applications*, vol. 2, p. 340, 2011.
- [15] T. Ohgaki, N. Ohashi, H. Kakemoto, S. Wada, Y. Adachi, H. Haneda, *et al.*, "Growth condition dependence of morphology and electric properties of ZnO films on sapphire substrates prepared by molecular beam epitaxy", *Journal of Applied Physics*, vol. 93, pp. 1961-1965, 2003.
- [16] Y. Ryu, S. Zhu, J. Budai, H. R. Chandrasekhar, P. F. Miceli, and H. White, "Optical and structural properties of ZnO films deposited on GaAs by pulsed laser deposition", *Journal of Applied Physics*, vol. 88, pp. 201-204, 2000.
- [17] W. J. Aziz, R. S. Sabri, and A. K. Jarallah, "Production of TiO₂ nanoparticles in different phases and shapes by using PLA and hydrothermal method", *Al-Mustansiriyah Journal of Science*, vol. 29, p. 4, 2018.
- [18] R. A. Ismail, N. F. Habubi, and A. N. Abd, "Effect of laser fluence on the characteristics of CdSe nanoparticles prepared by laser ablation in methanol", *High Energy Chemistry*, vol. 49, pp. 438-448, 2015.
- [19] B. R. Ali, "Synthesis And Characterization Of Nanoparticles Mgo Films On Silicon Substrates For Solar Cells Applications", *Synthesis*, vol. 2, 2016.
- [20] A. Al-Haddad, Z. Wang, M. Zhou, S. Tarish, R. Vellacheri, and Y. Lei, "Constructing Well-Ordered CdTe/TiO₂ Core/Shell Nanowire Arrays for Solar Energy Conversion", *Small*, vol. 12, pp. 5538-5542, 2016.
- [21] M. Guo, P. Diao, and S. Cai, "Hydrothermal growth of well-aligned ZnO nanorod arrays: Dependence of morphology and alignment ordering upon preparing conditions", *Journal of Solid State Chemistry*, vol. 178, pp. 1864-1873, 2005.
- [22] G. Xiong, U. Pal, J. Serrano, K. Ucer, and R. Williams, "Photoluminescence and FTIR study of ZnO nanoparticles: the impurity and defect perspective", *physica status solidi c*, vol. 3, pp. 3577-3581, 2006.
- [23] M. Faisal, S. B. Khan, M. M. Rahman, A. Jamal, K. Akhtar, and M. Abdullah, "Role of ZnO-CeO₂ nanostructures as a photo-catalyst and chemi-sensor", *Journal of Materials Science & Technology*, vol. 27, pp. 594-600, 2011.
- [24] R. Salehi, M. Arami, N. M. Mahmoodi, H. Bahrami, and S. Khorramfar, "Novel biocompatible composite (chitosan-zinc oxide nanoparticle): preparation, characterization and dye adsorption properties", *Colloids and Surfaces B: Biointerfaces*, vol. 80, pp. 86-93, 2010.
- [25] A. Niemegeers and M. Burgelman, "Effects of the Au/CdTe back contact on IV and CV characteristics of Au/CdTe/CdS/TCO solar cells", *Journal of Applied Physics*, vol. 81, pp. 2881-2886, 1997.